1. AGENCY USE ONLY (Leave blank)	2. REPORT DATE	3. REPORT TYPE AND DATES COVERED
	10/22/96	Final: 5/95 - 5/96

4. TITLE AND SUBTITLE
Micro-Mechanisms of Corrosion Fatigue Using Atomic Force Microscopy at Active Microstructural Sites on 2024-T3 Aluminum

5. FUNDING NUMBERS
~~F49620-92-J-0019~~
F49620-95-1-0334

6. AUTHOR(S)
Campbell Laird, Ph.D.
John J. DeLuccia, Ph.D.

7. PERFORMING ORGANIZATION NAME(S) AND ADDRESS(ES)
Univ of Pennsylvania
133 South 36th St., Suite 300
Philadelphia, PA 19104-3246

8. PERFORMING ORGANIZATION
AFOSR-TR-96 97
0065

9. SPONSORING/MONITORING AGENCY NAME(S) AND ADDRESS(ES)
AFOSR/NE
Building 410, Bolling AFB DC
20332-6448

AGENCY REPORT NUMBER

11. SUPPLEMENTARY NOTES

12a. DISTRIBUTION/AVAILABILITY STATEMENT
APPROVED FOR PUBLIC RELEASE; DISTRIBUTION IS UNLIMITED.

12b. DISTRIBUTION CODE

13. ABSTRACT *(Maximum 200 words)*

This is a final report summarizing a one-year effort to define the micro-mechanisms of corrosion fatigue of 2024-T3 sheet aluminum alloy in low pH environments using in-situ and ex-situ instrumentation, e. g., atomic force microscopy (AFM), scanning electron microscopy, and Auger spectroscopy. Constant stress, flexure fatigue specimens cycled in a unique mechanically driven, environmentally controlled, deformation stage, are electrochemically polished to exhibit uniform quality metallographic surfaces. Pertinent surface microstructural features of crack nucleation were determined by AFM on specimens fatigued in air, .01 M and 0.1 M HCl. Imposed cathodic polarization potentials during corrosion fatigue indicate a hydrogen embrittlement contribution to the fatigue process at potentials not affording sufficient cathodic protection. Enhanced embrittlement (~40% decreased in cycles to failure) was observed when 1.5 mg/ml of $NaAsO_2$ was added to 0.1M HCl solution at open circuit voltages (freely corroding). Other results from the subject program previously reported in the open literature are referenced here, but not reported again.

19970128 179

14. SUBJECT TERMS
Corrosion, aluminum-copper alloys, fatigue, corrosion fatigue, hydrogen embrittlement, atomic force microscopy, intergranular cracking, persistent slip bands.

15. NUMBER OF PAGES
43

16. PRICE CODE

17. SECURITY CLASSIFICATION OF REPORT	18. SECURITY CLASSIFICATION OF THIS PAGE	19. SECURITY CLASSIFICATION OF ABSTRACT	20. LIMITATION OF ABSTRACT
UNCLASSIFIED	UNCLASSIFIED	UNCLASSIFIED	

UNIVERSITY of PENNSYLVANIA

School of Engineering and Applied Science
Department of Materials Science and Engineering
Philadelphia, PA 19104-6272
215-898-6664

Campbell Laird
Professor

October 23, 1996

Dr. Charles Ward
AFOSR/NC
110 Duncan Avenue
Suite B115
Bolling AFB, DC 20332-0001

Re: Final Report - F49620-92-J-0019

Dear Chuck:

Please find enclosed our final report for the subject grant. Note that we have not repeated any material already reported in our previous publication. This is all new stuff. The results on hydrogen embrittlement during fatigue of 2024 alloy must be very interesting to the AF and I urge your close attention to them. We have even more material recently completed (the student took his defense - very successfully - today) and will be preparing other publications in the near future. Stay tuned!

It is very disappointing not to be able to proceed with this work when the start has been so promising. However, we enjoyed the work and greatly appreciate your support. John DeLuccia joins me in sending our warm thanks.

Sincerely,

Campbell

Campbell Laird

cc: John DeLuccia

Micro-Mechanisms of Corrosion Fatigue Using Atomic Force Microscopy at Active Microstructural Sites on 2024-T3 Aluminum

1.0 Introduction

It has been known for decades that the fatigue and fracture behavior of materials depends strongly on the nature of the chemical environment (see 1-4 for review). Even air is not an inert environment and fatigue lives can be drastically reduced in the presence of an aggressive environment in comparison to behavior in vacuum. High strength materials are particularly vulnerable to corrosion fatigue and their fatigue strength levels can be reduced to dangerously low levels. This is especially critical for Aerospace alloys [5-7]. The tendency of hard materials to fracture easily in hydrogen and other forms of environmental embrittler even for static loading is notorious.

Because of the dangers of corrosion fatigue and the role of environment in fracture, much effort has been spent in studying these problems. However, there are so many factors involved and the operative mechanisms so variable and complicated, that general understanding is either difficult or impossible to obtain, or simply inappropriate. Most of the research studies dealing with fatigue have been concerned with the kinetic effects of the environment, cyclic stresses and cyclic stress intensities (ΔK) on the nucleation and growth of fatigue cracks. The group of fatigue workers at the University of Pennsylvania has taken the path of studying the interactive effects of corrosion and cyclic deformation, and particularly the role of aggressive environment in affecting localized strain.

Research at the University of Pennsylvania has dealt with changes in strain localization behavior induced by fatigue in both inert environments [8,9] and aggressive environments [10-23]. The aggressive environments have been of the aqueous variety, and have involved both those which prevent oxide formation [10-15] and those which encourage it [13-15, 18-20].

The development of the Atomic Force Microscope (AFM) offers a way to overcome the difficulties of traditional techniques used to assess corrosion fatigue, by permitting direct observation of surfaces in fatigued metals at the level of nm resolution, while the surfaces are simultaneously exposed to corrosive environment. It is now conceivable that the simultaneous action of the environment and the stress will allow for direct imaging. Since the greater part of fracture-sensitive phenomena occurs at the surface in fatigue, the development of the AFM provided an outstanding opportunity for increasing our understanding of fatigue and corrosion fatigue. AFM was used to analyze morphologies at changing interfaces and to uncover fundamental stress-environmental related phenomena in the commercial aluminum alloy 2024-T3.

1.1 Description of AFM

The AFM gives topographic images by scanning a sharp stylus over a surface. It has the capability of producing surface images with atomic resolution on both conductors and non-conductors which offers an advantage over scanning tunneling microscopy (STM) and scanning electron microscopy (SEM) in that the sample need not be a conductor. Furthermore, the AFM offers the unique capability that it performs even better under liquid environments than it does in gas

or air environments. The AFM consists of a stylus that is attached to a cantilever which has a spring constant (0.1 -- 1 N/m) that is significantly less than the spring constant between atoms on the surface of a solid (10 N/m). Forces as small as $7x10^{-10}$ N can be held constant between the stylus tip and the surface. Operating with such small forces offers the ability to probe the surface without damaging or distorting the surface atomic and/or molecular topography. The surface is scanned under the stylus and the cantilever is deflected as the electron wave functions (EWF) of the stylus tip atoms interact with the EWF of the surface atoms. Images are produced by measuring the deflection of the cantilever as the stylus is scanned across the surface.

1.2 Corrosion of 2024-T3

Corrosion of aluminum alloys has been mostly investigated in natural sea water environments or in 3.5% NaCl solutions. Investigations into the corrosion behavior of naturally aged 2024 (T3 treatment) have shown that this alloy is susceptible to pitting and intergranular corrosion [21,22]. It has been experimentally verified that during localized corrosion of aluminum in neutral solutions there is a significant difference between the composition of the electrolyte in actively corroding regions (pits, grain boundaries) and the bulk of the electrolyte. Local electrochemical action lowers the pH of the electrolyte and creates concentrated acidic solutions within occluded corroding areas [22, 23, 24, 25]. In this work we describe the morphological changes of the surface of 2024-T3 aluminum alloy immersed in hydrochloric acid solutions. This alloy is known to undergo an acidic type of corrosion in chloride containing media [23,

24, 25]. The morphological changes leading to intergranular corrosion and the role of the second phase precipitates are explored.

1.3 Corrosion Fatigue of 2024-T3

The AFM offers a unique opportunity to explore the governing mechanistic features by permitting direct observation of surfaces in fatigued metals at the level of nm resolution while the surfaces are simultaneously exposed to corrosive environments. AFM imaging is used to catalog progressive changes occurring on the surface of the alloy during different stages of fatigue and corrosion fatigue. AFM images show the nature of corrosion in the vicinity of second phase particles which can lead to corrosion cracks along grain boundaries. Morphological investigations are also performed on surfaces resulting from samples dynamically stressed in air and hydrochloric acid environments. After AFM imaging, scanning electron microscopy is performed to provide analyses of the compositional variation on the surface and to compare the morphological features with those observed by AFM. The morphological interaction of fatigue damage, in the form of extrusions, cracks and steps, with corrosion damage are observed and interpreted.

1.4 Embrittlement of 2024-T3

In most aluminum alloys such as 1xxx (commercially pure aluminum), 5xxx (aluminum magnesium based alloys), and 7xxx (aluminum zinc based alloys), corrosion fatigue and stress corrosion cracking are believed to be hydrogen induced [26, 27]. The hydrogen embrittlement model postulates that atomic hydrogen is absorbed and somehow weakens the grain boundaries, which allows cracking [26]. However, for aluminum-copper based alloys (2xxx series), most

researchers accept an anodic dissolution model of stress corrosion and corrosion fatigue cracking [26, 28, 29]. This model assumes that cracking is due to the preferential dissolution along grain boundaries [29]. It has been recently reported that hydrogen embrittlement might play a significant role during stress corrosion of aluminum copper alloys [30, 31]. Since 2024-T3 is widely used for aerospace purposes and is known to undergo acidic corrosion in media containing chloride ions [32, 33], it is important to understand the corrosion mechanism and the influence of corrosive environments, including embrittlement, on its fatigue strength.

2.0 Experimental

2.1 Experimental Procedures for Corrosion Testing

2.1.1 Specimen and Solution Preparation

Aluminum (2024-T3) specimens (diameter 1/2") were cut from 1/8" thick sheet. The hardness of the 2024-T3 aluminum alloy was determined to be R_B 78 using a Wilson Rockwell tester with 1/16" diameter ball. The specimens were mechanically polished in a series of steps starting with fine-grained abrasive paper and followed with slurries of various alumina powders (5, 1, 0.3, and 0.05 μm). The mirror-like surfaces obtained were swab-etched in Keller solution (1.5 vol. % HF, 3.5 vol. % HCl, and 95 vol. % H_2O) for 5 to 15 seconds, rinsed in distilled water, repolished with 0.05 μm alumina powder, rinsed in distilled water and ethanol, and dried. To remove the amorphous surface oxide layer, specimens were electropolished in 64.5 vol. % acetic anhydride (Fisher Scientific, 99.2%) and 34.5 vol. % perchloric acid (Fisher Scientific, 70%) for 10 minutes (current density: 5 -- 10 mA/cm^2, voltage: 70 to 80 V), washed in deionized

water and ethanol, and dried. Immediately before each experiment, each specimen was degreased using acetone, wiped with Thompson lens paper, rinsed with distilled water and dried.

Aqueous solutions of 0.01 M and 0.1 M HCl were prepared by diluting a standard solution of 1.005-0.995 N HCl (Fisher Scientific) with deionized ultra-filtered water (Fisher Scientific).

2.1.2 AFM Imaging During Corrosion (*In Situ*)

AFM Experiments were performed with a Nanoscope II (digital Instruments, Inc.) using a 120 m scanner in the standard contact mode. A standard, commercially available fluid cell was used [34]. The cell volume was about 0.1 ml. The amount of electrolyte is quite small, and it may therefore undergo considerable changes in electrolyte concentration and pH during long immersion times. *In situ* experiments typically lasted between 6 to 40 hours, during which time the solution was replaced every 2 hours to minimize the evaporation of solution through the inlet and outlet ports, remove evolved hydrogen, and minimize the concentration variation of the solution throughout the experiments. This procedure insures that the variations in the pH of the solution are small. During the 2 hours of exposure, the pH of the solution changed from 0.0 to 0.3, from 1.0 to 1.20 -- 1.25, and from 2.00 to 2.15 -- 2.20, for 1 M HCl, and 0.01 M HCl solutions, respectively. Measurements of pH were performed before injection and after withdrawal of the solution from the AFM wet cell using a Piccolo 1280 pH electrode. Continuous replenishing of the corrosive solutions with a cell of this design was not possible because of persistent leakage problems.

Images were recorded at scan rates of 5 to 10 Hz. After collecting the images for the given immersion time, the AFM imaging system was disengaged and the tip was withdrawn from the surface (40-80 μm above the surface) to minimize the influence of the AFM tip on the electrochemical processes. The surface potential was not controlled. Various rotation angles and scan magnifications were applied and, except as noted, no obvious artifacts were observed to be caused by the tip presence or its geometry. For surface regions with high surface roughness, a strong convolution between the tip shape and surface feature shapes was observed. It is important to emphasize that many surface protrusions (e. g. slower dissolving regions, second phase precipitates) showed pyramidal shapes which in fact were the result of mimicking the shape of the AFM tip. In several cases soft corrosion products were dislodged from the sample surface by the scanning process. When this occurred, straight streaks (lines of uniform height) were observed in the AFM images along the scanning direction. In all cases disturbance of the corrosion products could be avoided by reducing the force between the tip and the sample surface.

Experiments for each concentration of HCl were performed on at least three different samples to insure the reliability of the observed morphological changes.

2.1.3 Ex Situ Characterization After Corrosion

After termination of the *in situ* experiments, all samples were removed from the AFM wet cell, washed in deionized water, dried, and subjected to scanning electron microscopy (SEM, JEOL 3000) analysis. SEM and *ex situ* AFM were used to verify the reliability of

the observed morphology for the other surface regions. Furthermore, energy dispersion X-ray analysis (EDX) was used for qualitative compositional analysis of the different surface regions during SEM observations, and Auger electron spectroscopy for quantitative compositional analysis.

After compositional analysis was performed on the numerous surface regions, the surface layer was removed by sputtering with argon ions to remove contamination due to the corrosive environment. A typical sputtering rate was about 20 nm/minute. After sputtering, composition analysis was performed on the different surface regions to determine the bulk composition of the observed surface features. A 10 kV beam voltage was used, and the Auger electrons were detected in the energy window between 30 to 1500 eV.

2.2 Corrosion Fatigue Experiments

2.2.1 Fatigue in Air, Distilled Water, and HCl Solutions

Aluminum (2024-T3) specimens were prepared from 1/8" thick sheet in the form of cantilever beam samples for fatigue and corrosion fatigue studies, or circular samples with a 1/2" diameter for corrosion investigations. Specimens were mechanically and electrochemically polished prior to experiments. Aqueous solutions of 0.01 M and 0.1 M HCl were prepared by diluting a standard solution of 1.005-0.995 N HCl (Fisher Scientific) with deionized ultra-filtered water as previously described.

Mechanical deformation test were performed in an alternate bending geometry. A unique mechanically driven deformation stage has been designed and constructed for this purpose. The specially

designed holders eliminate all tensile and compression stresses except those due to bending. For the cantilever beam samples, uniform strains in the range of 0.01% - 0.6% may be applied (~~Fig. 1~~) at a cyclic frequency variable from 0.01 Hz to 1 Hz. A special liquid cell has been designed to perform fatigue experiments in corrosive environments. It has not been found possible to apply stress while the AFM is actually in observational mode because bending amplitudes are too large. However, imaging can be carried out between strain excursions without specimen removal from the solution.

AFM imaging of the surface was carried out while specimens were fatigued in air, distilled water, 0.01 M HCl and 0.1 M HCl solutions. *In situ* corrosion AFM experiments were performed with a Nanoscope II (Digital Instruments, Inc.) using a 120 μm scanner. a standard fluid cell was used. Additional description of the fluid cell has been presented elsewhere. [35]

Fatigue and corrosion fatigue AFM studies were performed with a Dimension 3000 (Digital Instruments, Inc.) using a 120 μm scanner. Typical experiments lasted between 4 to 60 hours. AFM morphological investigations were performed in the same, well-defined cycle intervals of the fatigue lives, i. e., before mechanical deformation, after 100 cycles, 200 cycles, 500 cycles, and then in 1,000 or 5,000 cycle intervals depending on the strain amplitude, and at the end of the cyclic life. All AFM images were obtained after stopping the mechanical deformation. The computer-controlled stage of the Dimension 3000 microscope allows automatic localization of the surface region within an error less than 10 μm. This makes it

possible to observe the progressive changes in the same region of the specimen surface.

After termination of the *in situ* experiments, samples were removed from the wet cell, washed in deionized water, dried, and subjected to scanning electron microscopy (SEM, JEOL 3000) analysis. SEM and *ex situ* AFM were used to verify the reliability of the observed morphology for the other surface regions. Furthermore, energy-dispersive X-ray analysis (EDX) was used for qualitative compositional analysis of the different surface regions during SEM observations.

2.2.2 Polarization Behavior

Anodic and cathodic polarization behaviors of the alloy in 0.1 M HCl solutions were obtained by conventional D. C. potentio dynamic polarization techniques using a PAR potentiostat. A typical potential - log current plot for the alloy is shown in Figure 1. Figure 2 shows the resulting polarization behavior when the alloy is subjected to 0.1 M HCl containing 1.5 μg/ml of sodium arsenite, $NaAsO_2$. The arsenic compound is known to retard the hydrogen evolution kinetics in most metals experiencing cathodic reactions and thus often results in increased hydrogen entry into the metal, enhancing embrittlement.

2.2.3 Fatigue in 0.1 M HCl at Open Circuit Potentials and Imposed Cathodic Potentials

The experimental technique for the fatigue testing of the freely corroding (at open circuit potential) alloy in 0.1 M HCl was previously described in 2.2.1.

Fatigue tests were carried out on the alloy in 0.1 M HCl while being polarized at constant cathodic potentials. The chosen

polarization potentials were: -600 mV, -700 mV, -800 mV, and -900 mV. All reported potential values are versus the saturated calomel electrode (SCE).

2.2.4 Fatigue in 0.1 M HCl Containing $NaAsO_2$

Fatigue tests were carried out on the alloy in .01 M HCl containing 1.5 μg/ ml of Na_2AsO_2 at open circuit (freely corroding) and at -700 mV versus SCE.

2.2.5 Fatigue of Pre-Corroded Specimens in Air and Acid Environments

Fatigue specimens of the alloy were corroded in the unstressed condition by exposure to 0.1 M HCl solution for 6 hours. Some specimens were rinsed in fresh water, allowed to dry, then tested by fatigue in air. Some specimens were tested in fatigue immediately after pre-corrosion while still in the 0.1 M HCl. Some specimens were tested in the acid containing 1.5 μg/ml $NaAsO_2$.

The surfaces of other pre-corroded specimens were rinsed and then etched in concentrated HNO_3 to remove any copper deposits caused by the pre-corrosion. These specimens were subsequently fatigue tested in air and in 0.1 M HCl with and without arsenic additions.

3.0 Results

The results of the research described in 2.1.2 and 2.1.3 are documented in the *Journal of the Electrochemical Society,* vol. 143, no. 8, August 1996, p. 2471.

The results of the research described in 2.2.1 are documented in *Materials Research Society Symposium Proceedings,* vol. 409, 1996, p. 201.

Additionally, the fatigue results (cycles to failure) resulting from testing in distilled water at 0.2% strain level, reverse bending, were: 115,500; 125,000 and 121,900.

3.1 Polarization Behavior Results

D. C. polarization experiments are often used to categorize and quantify a metal's general corrosion tendency in a given environment. Anodic and cathodic polarization curves are used to determine the corrosion current usually by Tafel extrapolation. Figures 1 and 2 exhibit this behavior for the alloy in 0.1 M HCl and in 0.1 M HCl with arsenic additions. It is noted that the corrosion current, as determined by Tafel extrapolation, is smaller in the solution containing the arsenic compound. This could be a result of the ability of arsenic to form a surface film, thus reducing the area for surface dissolution. This is corroborated by Auger spectroscopy experiments showing the presence of the redeposited copper existing in the combined state (not elemental) constituting a surface film. This is shown in Figure 3, where a copper peak shift is noted with arsenic upon sputter etching the surface. It is pointed out that D. C. polarization methods are of minimal value in predicting the contribution of environmental effects on fatigue lives of aluminum alloys. D. C. methods are indicative of an overall electrochemical response of the alloy in the specific environment. In corrosion fatigue, where cracking is environmentally nucleated, (pits and intergranular trenches), and propagated, (a crack growing in a wet environment through embrittled metal), the governing events at the tip of the crack are not shown by ordinary D. C. methods. This explains the observation that the lowering of fatigue resistance in

environments containing arsenic compared to those without arsenic. The arsenic tends to increase embrittlement of the metal even while slightly decreasing the overall dissolution rate.

3.2 Results of Corrosion Fatigue at Open Circuit Potentials and at Imposed Polarization Potentials

It is well known that aqueous environments have a detrimental effect on the fatigue lives of high strength alloys as previously described in this work (Materials Research Society Publication). Figure 4 shows this effect graphically in the reduction of fatigue lives when the alloy is exposed to progressively more aggressive environments during fatigue. The results of Figure 4 are detailed in Table 1.

Environment	Polarization Potential vs. SCE	Cycles to Failure (different samples)		
air	none	195,000	219,200	200,500
deionized water	none	115,500	125,000	121,900
0.01 M HCl	O. C. V. (free corrosion)	59,900	63,700	60,800
0.01 M HCl	-700 mV vs. SCE	67,800	69,400	70,700
0.1 M HCl	O.C.V.= -560 mV(free corrosion)	48,500	49,800	50,500
0.1 M HCl	-600 mV vs. SCE	46,200	46,800	48,000
0.1 M HCl	-700 mV vs. SCE	46,000	46,800	48,000
0.1 M HCl	-800 mV vs. SCE	56,000	55,500	59,500
0.1 M HCl	-900 mV vs. SCE	71,100	64,800	73,500
0.1 M HCl + As	O.C.V.= -550 mV(free corrosion)	30,200	32,000	33,200
0.1 M HCl + As	-700 mV vs. SCE	52,100	51,400	55,500

Table 1. Fatigue Life Data (constant amplitude, reverse bonding, 0.2% strain) in various environments and under various electrochemical potentials.

Table 1 also reveals the effect of imposed cathodic polarization potentials. Cathodic polarization imposes more active, anodic potentials on the surface of the alloy. This has the general electrochemical effect of minimizing natural anodic dissolution, i. e., corrosion. In order to totally stop corrosion, the surface would need to be polarized at the open circuit potential of the microanodes; a value for unfilmed aluminum of about -1.6 volts. Since these experiments only went as low as -900 mV, only partial cathodic protection was achieved. It is emphasized that hydrogen

embrittlement is a concomitant to cathodic polarization in acidic environments on most high strength alloys, aluminum included.

3.2.1 Deionized Water

The 40% decrease in fatigue life manifested by the mere exposure of the fatigued alloy to deionized water demonstrates the power of interaction of a seemingly innocuous environment on the fatigue life of the alloy. The fact that the persistent slip bands, PSBs, described in the aforementioned Materials Research Society publication, were emerging at a surface wet with pure water, afforded an opportunity for fresh (uncoated) material to go into solution (corrode) and leave behind the corrosion product aluminum hydroxide and hydrogen thusly:

$$Al + 3H_2O \rightarrow Al(OH)_3 + 3/2\ H_2.$$

The above reaction is also operative at the grain boundary areas where the copper-depleted zone and copper-rich precipitates exist. Thus crack nucleation at the grain boundaries is prevalent when this alloy is exposed to distilled water. The cracks now growing in an aqueous environment in the presence of hydrogen experience advanced growth.

3.2.2 Hydrochloric Acid Solutions

The data from Table 1 concerned with corrosion fatigue in 0.1 M hydrochloric acid solutions is summarized in Figure 5. Plotting cycles to failure versus the electrochemical potential at the surface, we note that the fatigue life decreases slightly from the freely corroding state (O. C. V.) when cathodically polarized at -600 and -700 mV. The fatigue life is seen to increase when the surface is polarized to -800 and -900 mV It can be inferred from these

observations that a corrosion and embrittlement mechanism is dominant at potentials above -700 mV to the O. C. V., and that partial cathodic protection exists at potentials below -700 mV. It should be noted that the principal cathodic reaction in these acid solutions is the reduction of hydrogen ions to hydrogen atoms.

Corrosion in acid solutions is usually characterized by hydrogen gas bubbles emanating from the corroding surface. Most (over 90%) of the reduced hydrogen atoms recombine to form hydrogen molecules, thus the diatomic gas, H_2 is formed. Those reduced H atoms that do not recombine are precisely those that remain adsorbed at the surface and are likely to be absorbed into the metallic lattice and cause embrittlement.

Thus the acid environment on this alloy facilitates fatigue crack nucleation by chemically providing pre-cracks at the grain boundaries, and aids propagation by lattice embrittlement caused by absorbed hydrogen atoms.

3.2.3 Hydrochloric Acid Solutions Containing Arsenic

It is well known that small additions of arsenical compounds to acid solutions enhance the entry of hydrogen in both steels and aluminum alloys.[36,37,38] The data in Table 1 show that the addition of 1.5 μg of sodium arsenite per milliliter of 0.1 M HCl solution reduced the fatigue life by 36% over that containing no arsenic. This is a clear indication of a hydrogen embrittlement contribution to the fatigue cracking process. When the specimen was cathodically polarized to -700 mV, the presence of arsenic did not enhance embrittlement and the fatigue life rose to slightly above that at open circuit containing no arsenic. This anomaly is yet to be fully

explained. The involvement of the re-deposited copper and its effect on hydrogen entry and its modification in the presence of arsenic is being considered. Recall, the presence of surface copper is modified in the presence of arsenic (see Figure 3).

3.3.3 Pre-corroded Specimens in Air, Acid Solutions and Cathodically Polarized in an Acid Solution

Fatigue and corrosion fatigue results in pre-corroded and pre-corroded and cleaned specimens compared to pristine specimens fatigued in the same environments proved interesting. The results of these experiments are shown in Table 2.

Condition Environment	Polarization Potential vs. SCE	Cycles to Failure (individual sample data)		
not pre-corroded 0.1 M HCl	none (O.C.V.)	48,500	49,800	50,500
Pre-corroded, not cleaned 0.1 M HCl	none (O.C.V.)	32,900	36,200	36,500
not pre-corroded 0.1 M HCl	-700 mV	43,500	44,900	46,000
Pre-corroded, not cleaned 0.1 M HCl	-700 mV	49,200	51,000	55,200
Not pre-corroded 0.1 M HCl + Arsenic	none (O.C.V.)	30,200	32,000	33,200
Pre-corroded, not cleaned 0.1 M HCl + As	none (O.C.V.)	33,000	34,500	36,900
Pre-corroded, cleaned 0.1 M HCl	none (O.C.V.)	40,500	41,300	44,200
Pre-corroded, cleaned 0.1 M HCl	-700 mV	38,200	40,100	41,400
Pre-corroded, cleaned 0.1 M HCl + Arsenic	-700 mV	26,000	27,100	29,400

Table 2. Corrosion Fatigue Life Data (constant amplitude, reverse bending, 0.2% strain) in various environments comparing pre-corroded and pre-corroded and cleaned specimens.

The data of Table 2 are summarized in Figures 6 and 7. From Figure 6, it is noted that pre-corrosion causes a large reduction (30%) in the fatigue life when the as-corroded specimens are fatigued in 0.1 M HCl. The fatigue life of the as-corroded specimens fatigued in 0.1 M and cathodically polarized to -700 mV actually increased (15%). A slight increase (10%) in the fatigue life was also noted for as-corroded specimens fatigued in 0.1 M HCl with a small addition of sodium arsenite, a hydrogen evolution reaction poison.

The 30% decrease in cycle life observed in 0.1 M HCl at O. C. V. was probably due to observed surface intergranular corrosion damage, and hydrogen absorption in pre-corroded specimens. When un-pre-corroded samples were exposed to corrosive environment, it took about 10,000 cycles before the first intergranular damage was observed at the sample surface. In the case of pre-corroded samples, strong intergranular damage already exists prior to corrosion fatigue testing; this results in the reduction of the life by the number of cycles needed for crack initiation in the case of an un-pre-corroded specimen. Furthermore, the hydrogen uptake as well as high stress concentration due to intergranular penetration are believed to contribute to the total 30% reduction of fatigue life.

It is interesting to note that fatigue life was observed to increase for pre-corroded un-cleaned specimens mechanically cycled in 0.1 M HCl at -700 mV vs. SCE as well as in 0.1 M HCl containing arsenic as compared with cycle life of un-pre-corroded samples under the same conditions. However, there was a layer containing a large amount of metallic copper present on pre-corroded and un-cleaned samples and this deposited copper can act as very efficient

cathodic site and preferentially reduce hydrogen and catalyze the hydrogen evolution reaction during fatigue. Due to a low diffusivity of hydrogen through copper, it can be expected that hydrogen reduced at these metallic copper regions would not enter the metal and thus contribute to the hydrogen embrittlement mechanism. Applying cathodic polarization under this circumstance results in some cathodic protection of the sample surface with minimal hydrogen entry during the pre-existing presence of copper, and therefore the observed increase in fatigue life.

Where the environment contains the catalytic poison arsenic, the slight rise in fatigue life could be caused by the anodic reaction inhibiting effect (lower corrosion current as shown in Figure 2) overshadowing the hydrogen embrittlement effect that would be enhanced by a hydrogen evolution poison. The preponderance of re-deposited copper could also serve to minimize the embrittlement effect.

Figure 7 demonstrates the results of a series of experiments performed on pre-corroded and cleaned specimens. Fatigue in 0.1 M HCl at O. C. V. resulted in a fatigue life of 42,000 cycles which is 15% shorter than that observed for un-pre-corroded samples and 20% longer than that observed for pre-corroded un-cleaned samples. This effect may be explained by considering that exposure to the concentrated nitric acid, an effective oxidizing agent, resulted in dissolution of the surface layer and re-enhancement of surface passivity (Al_2O_3). This would explain the slight beneficial effect on the corrosion fatigue performance of this alloy based on the following two reasons. First, cleaning removes inhomogeneities including

redeposited copper from the surface layer; therefore, the galvanic cell formation between grain boundaries and metallic copper deposit would not preexist. Second, a certain number of cycles would be required for passivity to breakdown during the exposure to corrosive environments. Therefore, the shortening of the cycle life as compared to corrosion fatigue of un-pre-corroded specimens would be mostly due to the mechanical effect of the intergranular damage introduced prior to mechanical straining, which results in higher stress concentrations, leading to higher effective strain at damaged regions. The longer lives observed for cleaned pre-corroded specimens, as contrasted with those of un-cleaned pre-corroded samples, would therefore be due to a less severe environmental interaction which leads to lower contribution of dissolution mechanism and hydrogen embrittlement.

From Figure 7 we also see that the fatigue of pre-corroded and cleaned specimens in 0.1 M HCl at -700 mV vs. SCE resulted in about 40,000 cycle life, which is10% shorter than the average life of un-pre-corroded samples and 25% shorter than those of pre-corroded un-cleaned specimens tested at exactly the same conditions. As compared to the cycle life for un-pre-corroded samples observed at O. C. V. conditions, applying cathodic polarization resulted in a 5% reduction of the cycle life for pre-corroded cleaned samples during corrosion fatigue. Furthermore, exposure to 0.1 M HCl solution containing arsenic resulted in the shortest lives observed for any corrosion fatigue test at any electrochemical condition, i. e., 27,500 cycles. This is about 15% shorter than the lives of un-pre-corroded

specimens deformed in the same environment and about 25% shorter than lives of pre-corroded and un-cleaned samples.

From the above results for pre-corroded and cleaned samples, it can be hypothesized that the same mechanism was observed as in the case of cyclic deformation of electrochemically polished, un-pre-corroded samples. That is, applying a cathodic potential of -700 mV vs. SCE resulted in lowering the anodic dissolution currents and enhancing the hydrogen entrance into the material now without redeposited surface copper. Addition of arsenic to the solution resulted in a similar effect; the dissolution current became smaller and the hydrogen uptake is enhanced due most likely to an increase in the normalized surface coverage. These results strongly suggest a detrimental role of hydrogen on the corrosion fatigue performance of 2024-T3 aluminum alloy. It may, therefore, be concluded that hydrogen enhanced cracking plays a significant role in the fatigue and fracture of this alloy. The mechanisms of both hydrogen embrittlement and anodic dissolution overlap, resulting in the reduction of the fatigue life of samples pre-exposed to aggressive environments.

Comparing the results of pre-corroded cleaned and un-cleaned samples, it appears that redeposited metallic copper, resulting from corrosion, controls the rate of hydrogen uptake by the material. For un-cleaned specimens, the corrosion fatigue life in 0.1 M HCl at -700 mV and in 0.1 M HCl with arsenic at O. C. V. increased as compared to those observed for un-pre-corroded samples. On the other, hand, removal of the copper-containing-surface-film resulted in a significant shortening of the cycle life under cathodic polarization of

-700 mV and in the environments containing arsenic, as compared to the result obtained for un-pre-corroded specimens. These results clearly indicate that metallic copper deposits act as the most important factor controlling hydrogen embrittlement of 2024-T3 aluminum alloy. Its presence in the metallic form in the surface film results in inhibition of hydrogen absorption, while the absence of metallic copper is seen to accelerate the hydrogen uptake of the material.

4.0 Summary

In the present study, the mechanisms of corrosion and corrosion fatigue of a 2024-T3 aluminum alloy in HCl solutions havebeen established. Dynamic mechanical tests were performed in a reverse bending mode at a constant strain amplitude. The effect of environment was investigated during free corrosion, e. g., at open circuit voltage (O. C. V.), and under different cathodic polarization potentials. Corrosive environments employed were 1.0 M, 0.1 M, and 0.01 M solutions of hydrochloric acid for corrosion studies, and 0.1 M HCl solutions containing no additive or 1.5 μg/ml of $NaAsO_2$ for corrosion fatigue studies. The *in situ* technique, electrochemical atomic force microscopy, was used for investigations of morphology changes on the sample surface in solutions during corrosion of this alloy and during the combined action of corrosive environments and cyclic mechanical straining (corrosion fatigue investigations.)

From the foregoing studies, the following phenomenologies were established and mechanisms proposed:

(1) The estimated corrosion current (Tafel extrapolation) for 2024-T3 exposed to 0.1 M HCl is 42 $\mu A/cm^2$. The estimated

corrosion current (Tafel extrapolation) for the alloy exposed to 0.1 M HCl with the addition of 1.5 μg/ml of $NaAsO_2$ is 18 $\mu A/cm^2$.

(2) Proposed mechanism of corrosion of a 2024-T3 aluminum alloy in HCl: after immersion in hydrochloric acid, the surface is attacked in specific areas where the passivity is vulnerable. After the passivity of the surface is destroyed, localized dissolution of the underlying matrix occurs, accompanied by strong hydrogen evolution at the cathodic sites. As soon as the more vulnerable regions of lower copper content are uncovered in the vicinity of the second phase precipitates, dissolution is accelerated along these paths, which leads to severe intergranular damage.

(3) During fatigue of a 2024-T3 aluminum alloy in air:

a) Only transgranular fracture was observed throughout the whole cyclic life.

b) For strain amplitudes larger than 0.4%, persistent slip bands (PSB's) form between large surface pits. After about 80% of the cyclic life, cracks nucleate and propagate along PSB's.

c) For strain amplitudes smaller than 0.4%, cracks nucleate along PSB's formed at the sample edges. The only observed crack is the fatal fracture crack, and fatigue damage is limited to the region in the vicinity of that crack.

(4) For samples fatigued in distilled water, accelerated crack nucleation occurs intergranularly in very early stages of fatigue life. This behavior is probably due to the presence of the copper depleted zones in the vicinity of the grain boundaries. The rupture of the

oxide film in these regions results in the immediate dissolution of copper depleted zones creating sites of dissolved materials which act as stress concentrators during subsequent cycles and results in the initial intergranular fracture. Furthermore, the hydrogen produced as a result of the corrosion reactions may enter the aluminum alloy and cause hydrogen embrittlement.

(5) During simultaneous exposure of a 2024-T3 aluminum alloy to mechanical deformation and an acidic environment, a large reduction in fatigue life has been observed. This can be attributed to the accelerated crack nucleation process and an embrittlement effect. The following phenomena were associated with this mechanism:

a) Dissolution of the regions along grain boundaries is accelerated by mechanical straining.

b) The surface cracks start out as intergranular ones, proceed intergranularly for a few grains and then change to a transgranular propagation mode.

c) Hydrogen embrittlement appears to play a role during corrosion fatigue of the 2024-T3 aluminum alloy in hydrochloric acid environments. This is suggested by cleavage-like fracture and secondary cracking observed in the early stages of transgranular crack propagation.

(6) The influence of hydrogen on the fatigue performance of this material is clearly demonstrated in experiments performed under cathodic polarization and in hydrochloric acid solution containing arsenic.

a) Shortening of cyclic life under cathodic polarization at -600 mV and -700 mV vs. SCE shows that at these cathodic potentials, hydrogen entry into the material is enhanced and results in hydrogen embrittlement of this alloy.

b) In solutions containing arsenic, the hydrogen combination reaction is poisoned; therefore, the atomic hydrogen adsorbed at the sample surface has ample time to diffuse into the material bulk and contribute to the fracture mechanisms. A 40% reduction of fatigue life was observed as compared to that in solutions without arsenic. Furthermore, the addition of arsenic to the solution was found to alter the surface chemistry of metallic copper redeposited on the sample surface. This drastic reduction in fatigue life is a strong endorsement of a hydrogen embrittlement mechanism associated with this alloy.

(c) A significant difference in the trend of cyclic life during corrosion fatigue under different electrochemical conditions was observed on pre-corroded samples. The presence of a copper-containing surface layer resulted in a lower contribution of hydrogen in the fracture mechanism. This is manifested by a longer cyclic life of samples covered with the copper-containing film as compared to those from which the film was removed prior to corrosion fatigue experiments.

(7) Based on this study the following mechanisms of corrosion fatigue and hydrogen embrittlement of a 2024-T3 aluminum alloys are proposed:

a) Fatigue cracks nucleate in the early stages of cyclic life during fatigue in hydrochloric acid environments along copper depleted regions in the vicinity of second phase precipitates and grain boundaries due to a higher reactivity of these areas. This creates regions of high stress concentration and results in the localization of plastic deformation in the these areas. Furthermore, reduction of hydrogen ions in crevices of dissolved grain boundaries leads to hydrogen absorption and facilitates fracture of a 2024-T3 aluminum alloy especially in the early stages of crack propagation. Fatigue cracks start at the sample surface as intergranular ones, propagate intergranularly through a few grains and then change their propagation mode to transgranular. Both intergranular fracture and cleavage-like transgranular fracture with secondary cracking are observed on the fracture surfaces.

b) The 2024-T3 aluminum alloy is susceptible to hydrogen embrittlement under certain surface conditions.. The single most important factor controlling the hydrogen uptake by a 2024-T3 aluminum alloy, and therefore, hydrogen embrittlement of this alloy, is the redeposition of metallic copper during corrosion fatigue of this alloy

in hydrochloric acid environments. The presence of metallic copper in the surface film formed at the sample surface during corrosion fatigue of the 2024-T3 aluminum alloy inhibits the uptake of hydrogen. Metallic copper acts as a preferential site for proton reduction during corrosion fatigue; however, due to very low hydrogen diffusivity in copper, hydrogen ions reduced at these sites do not contribute to hydrogen embrittlement. When copper is either removed (cleaned) or is complexed by solution ions and is not present in its metallic form at the surface, e. g., in a solution containing arsenic ions, the hydrogen uptake is enhanced and significant reduction of cyclic life is observed. i. e., the alloy is embrittled by hydrogen.

REFERENCES

1. O. F. Devereux, A. J. McEvily and R. W. Staehle, eds., "Corrosion Fatigue," NACE, Houston, 1972.
2. R. P. Gangloff and D. J. Duquette, in Chemistry and Physics of Fracture, eds., R. M. Latanision and R. H. Jones, Martinus Nijhoff Publishers, 1987, p. 612.
3. P. M. Scott and R. A. Cottis, Environment Assisted Fatigue, EGF Publ., MEPL, 1990.
4. J. Magnin, in Fatigue '93, Eds., J. P. Bailon and J. I. Dickson, EMAS, Ltd., West Midlands, 1993, Vol. II, pp. 733-744.
5. R. J. H. Wanhill and J. J. DeLuccia, Environmental Fatigue of Aluminum Alloy Structural Joints, Proceedings of 7th International Light Metals Conference, Vienna, Austria, June 1981.
6. R. J. H. Wanhill, J. J. DeLuccia and M. Russo, Fatigue in Aircraft Corrosion Testing (FACT) Program, NATO-AGARD Report No. 713, 1989.
7. J. J. DeLuccia, Corrosion Contribution to Environmental Cracking Failures of Critical Aircraft Parts, 12th International Corrosion Congress, Symposium on Aircraft Corrosion, National Association of Corrosion Engineers Conference Proceedings, 1993 Vol. 5A, 1993, p. 3099.
8. D. E. Witmer, C. Laird and G. C. Farrington, Acta Met., 3 5 (1987) 1911.
9. D. E. Witmer, C. Laird and G. C. Farrington, Acta Met., 3 5 (1987) 1895.

10. B. D. Yan, G. C. Farrington and C. Laird, Fatigue 84 (1984) Vol. III, 1435.
11. B. D. Yan, G. C. Farrington and C. Laird, Met. Trans., 16A (1985) 1151.
12. B. D. Yan, G. C. Farrington and C. Laird, Acta Met., 33 (1985) 1533.
13. B. D. Yan, G. C. Farrington and C. Laird, Acta Met., 33 (1985) 1593.
14. B. D. Yan, G. C. Farrington and C. Laird, Fatigue Fracture Eng. Mat. and Structures, 8 (1985) 259.
15. B. D. Yan, E. Young, G. C. Farrington and C. Laird, Corrosion Science 26 (1986) 121.
16. S. Ortner, C. Laird and G. C. Farrington, Acta Met, 35 (1987) 453.
17. S. Ortner, C. Laird and G. C. Farrington, Acta Met, 35 (1987) 867.
18. S. Ortner, C. Laird and G. C. Farrington, Mat. Sci. Eng., 89 (1987) 45.
19. Z. Y. Zhu, G. C. Farrington and C. Laird, Mat. Sci. Eng., 91 (1987) 125.
20. H. Vehoff, C. Laird and D. J. Duquette, Acta Met., 35 (1987) 2877.
21. G. L. Sheider, N. N. Cherkasov, V. I. Smolentsev, B. E. Popov and A. P. Kovtun, Mat. Sci. Heat Treat., 26, 632 (1985).
22. H. Kaesche, Pitting Corrosion Aluminum and Intergranular Corrosion of Aluminum Alloys in Localized Corrosion, Houston, TX, NACE 1974, p. 516.

23. L. F. Mondolfo, Aluminum-Copper Alloys in Aluminum Alloys: Structure and Properties, Butterworths, London-Boston 1976.
24. L. L. Shreir, R. A. Jarman, and G. T. Burstein, Non-ferrous Metals and Alloys in Corrosion Vol. 1, Butterworths-Heinemann Ltd., London-Boston 1994.
25. R. T. Foley, Corrosion, 42, 277 (1986).
26. T. D. Burleigh, Corrosion, 47, 89 (1991).
27. T. Magnin, ISIJ International, 36, 223 (1995).
28. M. R. Bayoun, Engineering Fracture Mechanics, 45, 297 (1993).
29. K. Urushino and K. Sugimoto, Corrosion Science, 19, 225 (1979).
30. D. A. Hardwick, M. Taheri, A. Thompson, I. M Bernstein, Metall. Trans. A, 13, 811 (1982).
31. F. Zeides and I. Roman, Materials Science and Engineering, A125, 21 (1990).
32. H. Kaesche in Localized Corrosion, Houston, TX, NACE 1974, p. 516.
33. E. H. Hollingsworth and H. Y. Hunsicker in Metals Handbook Vol. 13, Corrosion.
34. K. Kowal, L. Xie, R. Huq and G. Farrington, J. Electrochem Soc., 141, 1166 (1994).
35. K. Kowal, J. DeLuccia, J. Josefowicz, C. Laird and G. Farrington, *In situ* Atomic Force Microscopy Observations of the Corrosion Behavior of Aluminum-Copper Alloys, J. Electrochem Soc., Vol. 143, no. 8, August 1996. p. 2471.
36. A. Tendulkar and T. Radhakrishnan, A Galvanostatic Study of the Role of Arsenic on the Entry of Hydrogen into Mild Steel, Corrosion Science, Vol. 36, no. 7, pp. 1247-1256, 1994.

37. T. Radhakrishnan and L. Shrier, Permeation of Hydrogen Through Steel by Electrochemical Transfer - I. Influence of Catalytic Poisons, Electrochimica Acta, 1966, Vo. II, pp. 1007-1024.

38. E. Smith and D. Duquette, Effect of Cathodic Polarization on the Corrosion Fatigue Behavior of a Precipitaion Hardened Aluminum Alloy, Metallurgical Transactions A, Vol. 17A, Feb. 1986, p. 339.

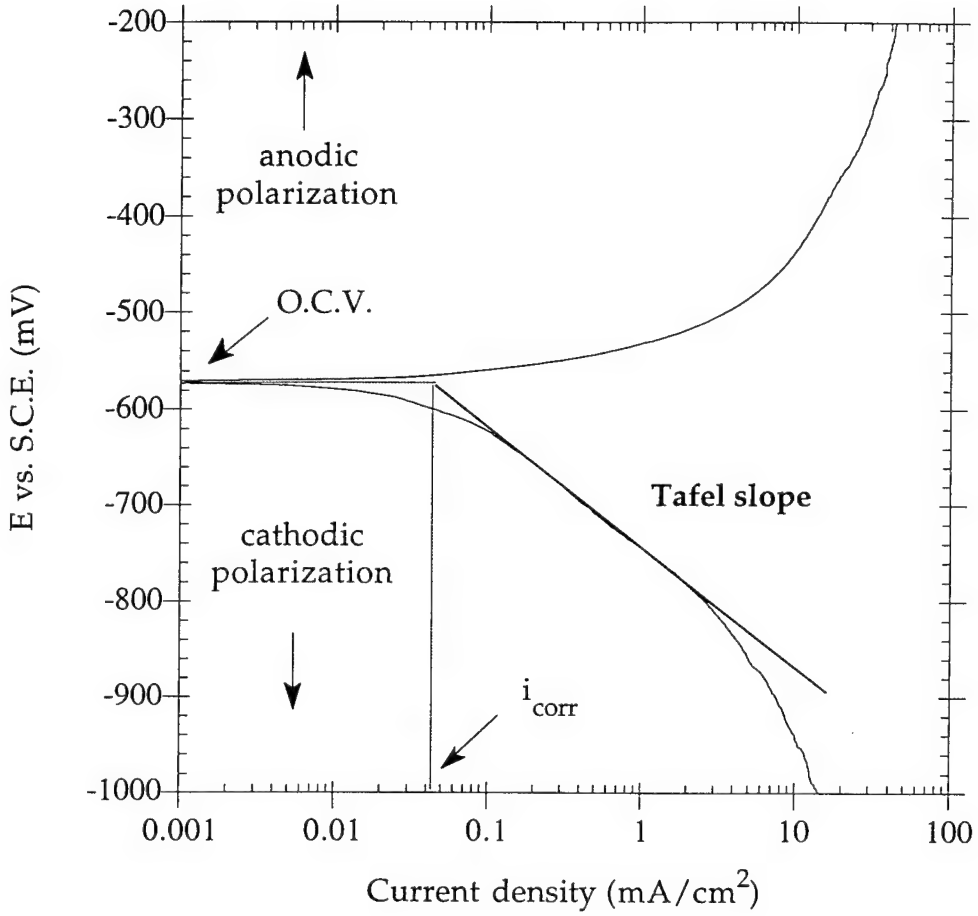

Figure 1. Anodic and cathodic polarization behavior of 2024-T3 Aluminum in 0.1M HCl at 25°C

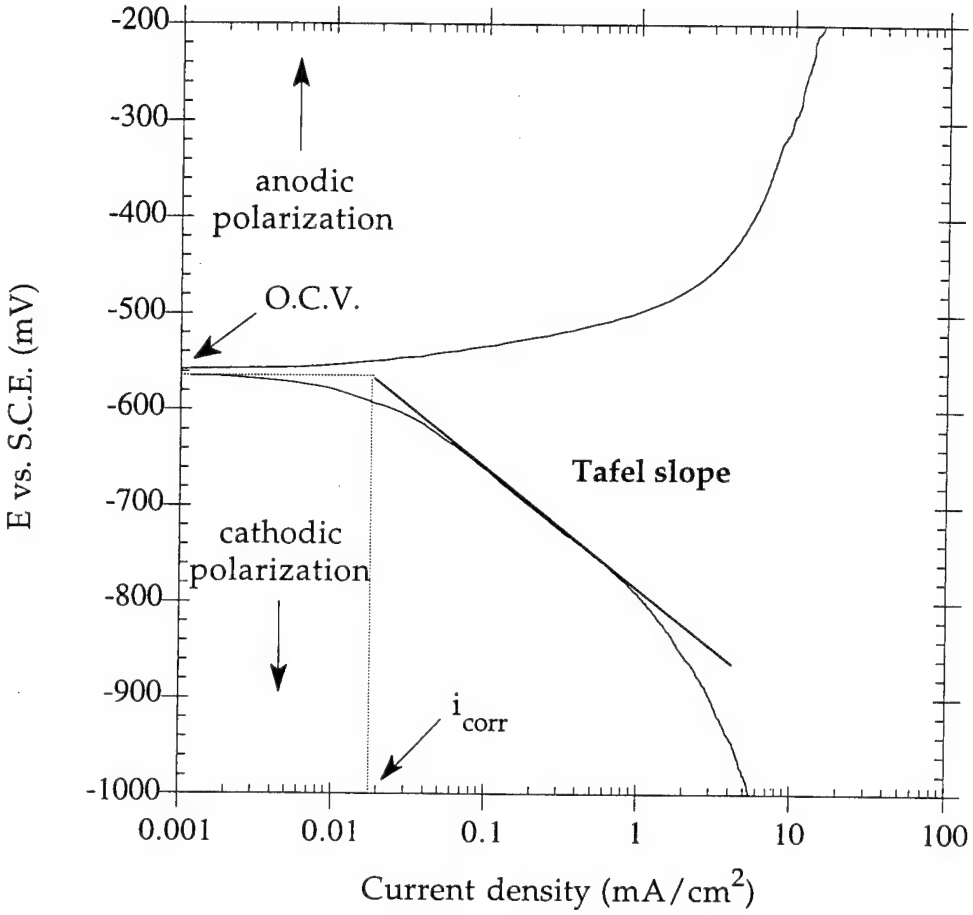

Figure 2. Anodic and cathodic polarization behavior of 2024-T3 Aluminum in 0.1M HCl containing 1.5 um.ml $NaAsO_2$ at 25°C

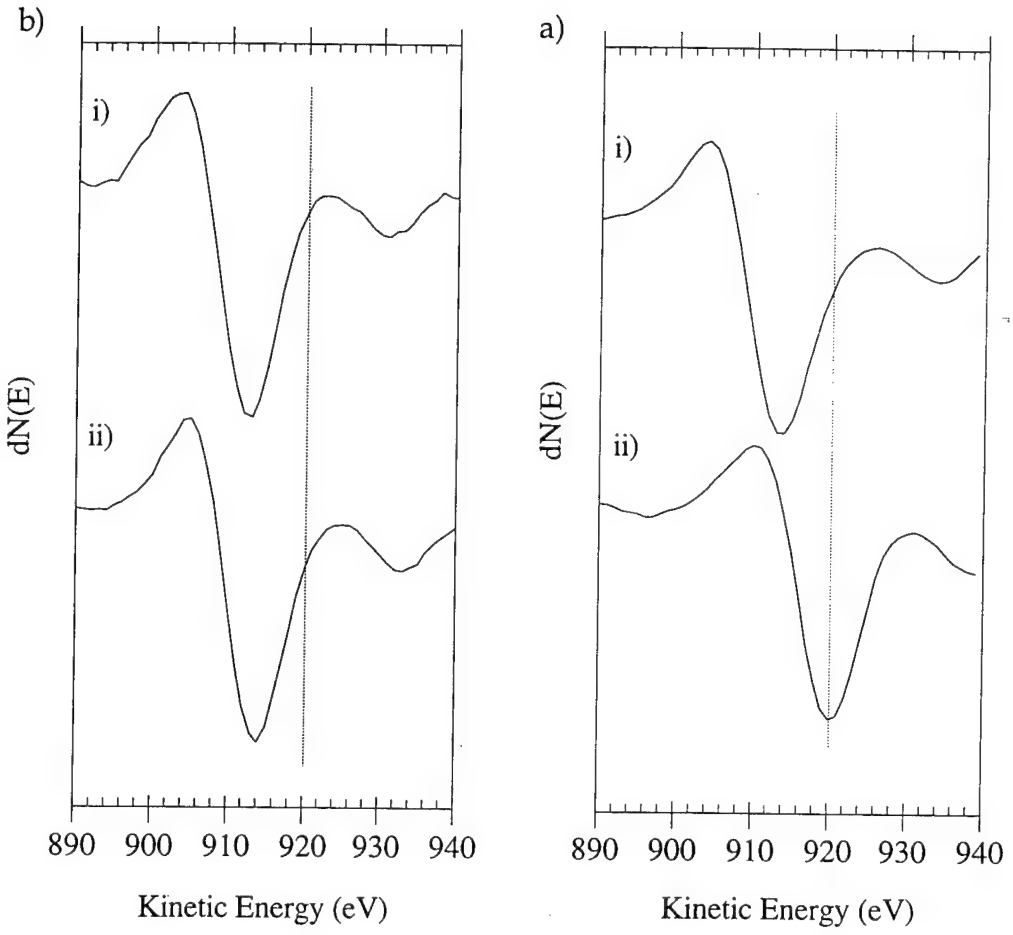

Figure 3. Aguer spectra of copper peaks
(a) 0.1M HCl, (b) 0.1M HCl + 1.5 um/ml of $NaAsO_2$
(i) unsputtered surface, (ii) argon sputtered (500 Å) surface

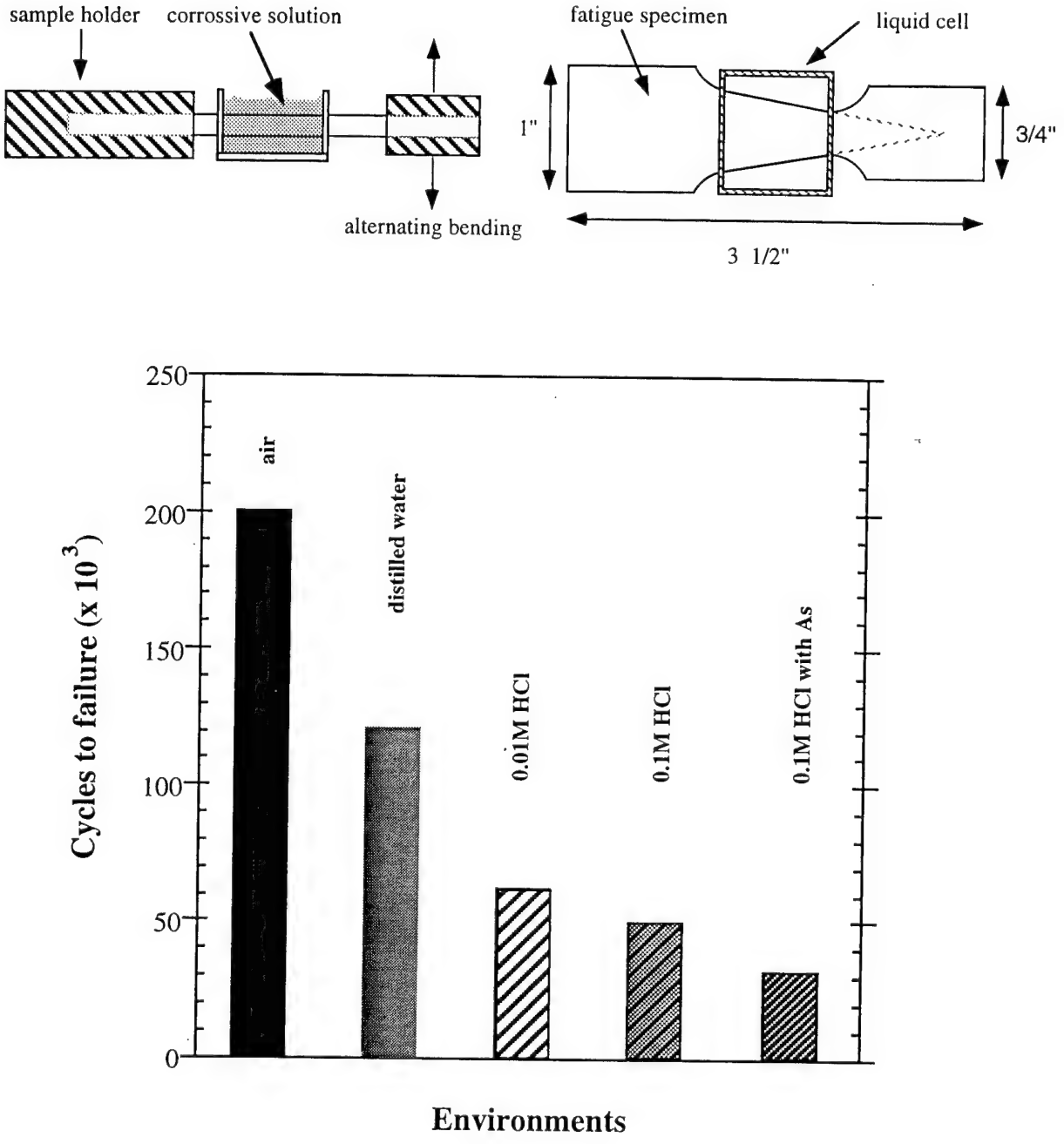

Figure 4. Fatigue life comparisons of 2024-T3 Aluminum in various aqueous environments; reverse bending, 0.2% strain.

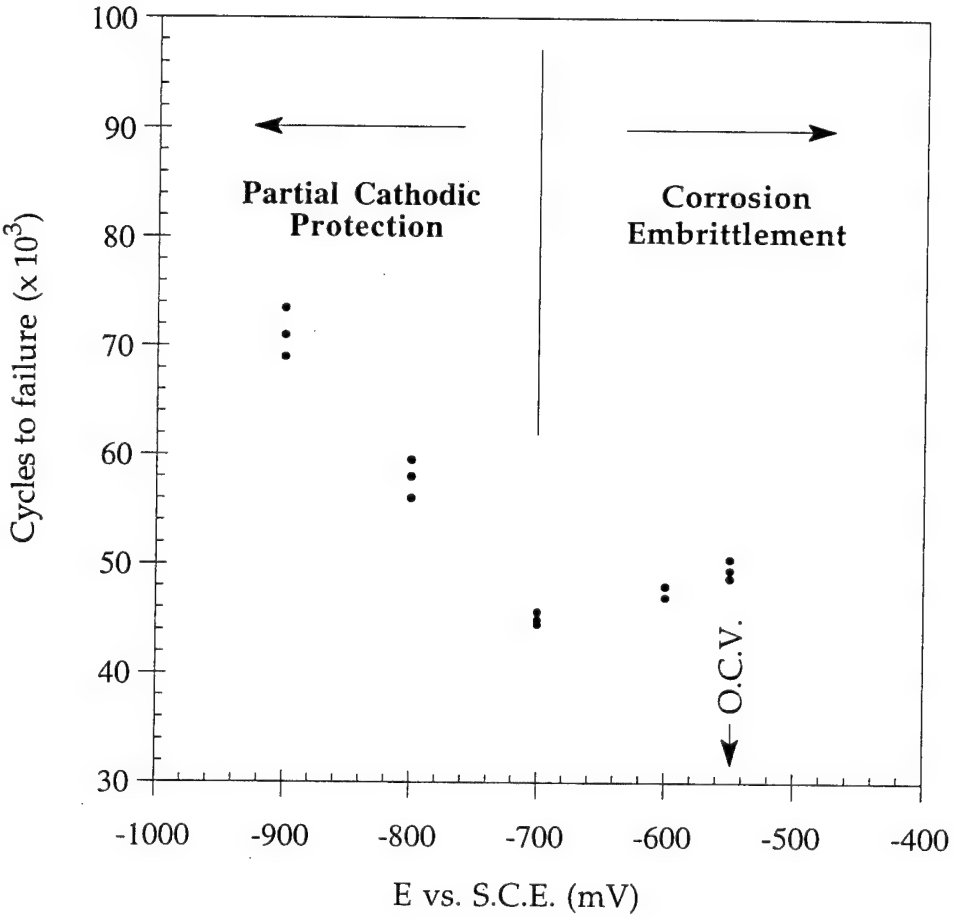
100
90
80
70
60
50
40
30
Cycles to failure (x 10^3)
Partial Cathodic Protection
Corrosion Embrittlement
O.C.V.
-1000
-900
-800
-700
-600
-500
-400
E vs. S.C.E. (mV)

Figure 5.

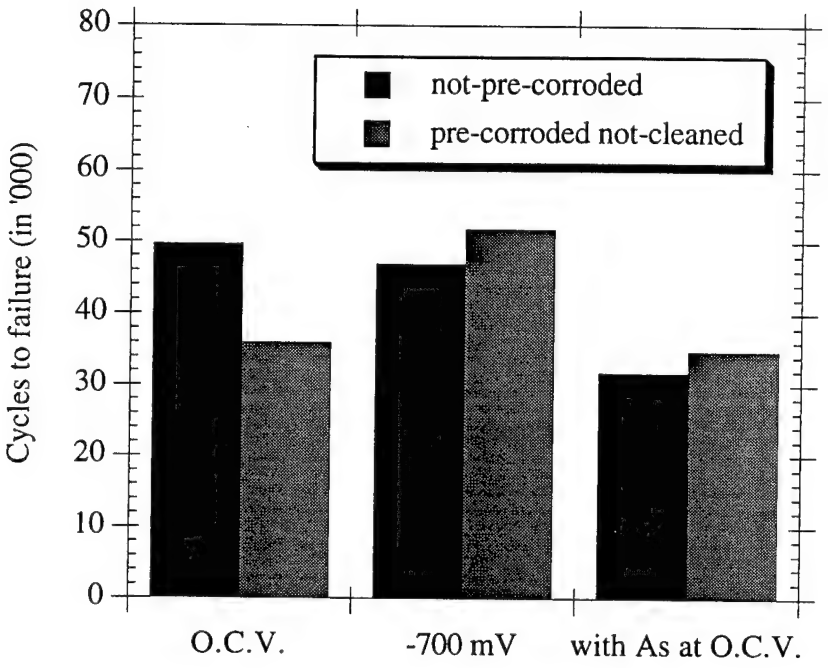

Figure 6. **Cyclic life of pre-corroded, un-cleaned samples in different environments; strain = 0.2%, f = 0.5 Hz.**

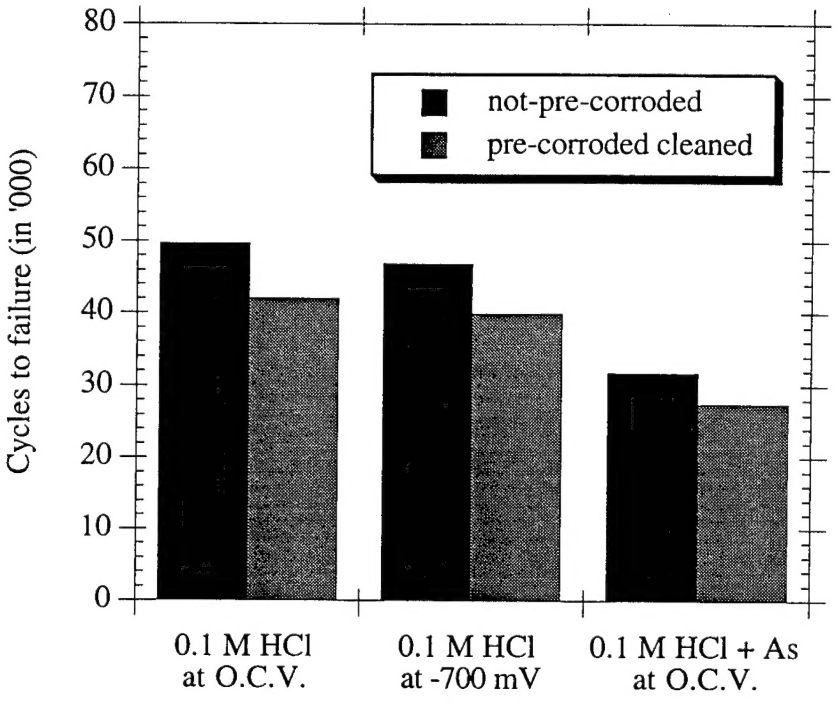

Figure 7. **Cyclic life of pre-corroded, HNO_3-cleaned samples in different environments; strain = 0.2%, f = 0.5 Hz.**

KEY PERSONNEL

Campbell Laird, Ph.D., P.E., FASM

Professor of Materials Science and Engineering, University of Pennsylvania, Philadelphia, PA. Dr. Laird obtained his degrees at the University of Cambridge and was appointed a Fellow of Christ's College, Cambridge. He then gained industrial experience at the Scientific Laboratory of the Ford Motor Co. for five years as a senior research scientist before returning to academic life, where he has since served for twenty-five years, including two terms as Chairman. He is credited with approximately 250 publications and a patent, and 45 graduate students have received Ph.D. degrees under his advisorship. His main areas of interest have covered fatigue and cyclic deformation, as well as phase transformations, but he has focused on corrosion fatigue for the last twelve years. Much of his research, including phase transformations, has been conducted on model and commercial aluminum alloys, and he has consulted for the aerospace industry for 21 years. He was awarded the Darwin prize for his thesis, two citations in the MITRE report and the outstanding papers award from ACTA Metallurgica.

John J. DeLuccia, PhD, FASM

Adjunct Professor of Materials Science and Engineering, University of Pennsylvania, Philadelphia, PA. Formerly Senior Materials Engineer, Aerospace Materials Division, Naval Air Warfare Center, Warminster, PA. Dr. DeLuccia has 33 years of experience with aerospace materials both as a scientist and as a manger. He is particularly active in the areas of aircraft corrosion and embrittlement research and was the principal investigator in a program that transferred aircraft corrosion control technology and training from the military (Navy) to the civilian sector (FAA). Dr. DeLuccia developed a three day short course for FAA inspectors and engineers and has taught courses in material science and engineering including electrochemistry and corrosion control theory at the undergraduate and graduate levels for the past 33 years. He is credited with 52 publications and holds three patents. Dr. DeLuccia received a PhD in Metallurgy and Materials Science from the University of Pennsylvania; he is a fellow of the ASM International; past Corrosion Subcommittee Chairman of AGARD-NATO; and is a 1994 recipient of the U.S. Navy's Meritorious Civilian Medal.

Gregory C. Farrington, PhD, D. Phil. (h.c.)

Dean, School of Engineering and Applied Science, University of Pennsylvania, Philadelphia, PA since 1990. Professor Farrington has seven years experience as a research scientist at the General Electric Company and sixteen years experience as a professor, center director, and dean at the University. He is an international authority on electrochemistry and materials science, with particular emphasis on electrochemical energy sources. Professor Farrington is credited with 127 publications, 10 books/chapters in books, and 27 patents. He is the recipient of many national and international awards and serves/chairs on numerous scientific, educational, and civic panels and boards. Professor Farrington received a PhD (Chemistry) from Harvard University as well as a D. Phil. (*honoris causa*) from the University of Uppsala, Sweden.

Jack Y. Josefowicz, PhD

Visiting Professor of Materials Science and Engineering, University of Pennsylvania and Senior Research Scientist, Hughes Research Labs, Malibu, California. Dr. Josefowicz has 20 years experience pursuing industrial research both fundamental and applied. His particular areas of expertise are: atomic force microscopy, electrochemistry, electronic and semi-conductive materials, and solid-electrolyte interfaces. In his short time at the University, Dr. Josefowicz established the atomic force microscopy laboratory, one of the few in the country that is capable of full range electrochemical and mechanical experimentation. He is credited with 45 publications and has issued 12 patents. Dr. Josefowicz received a Ph.D. (physics) from the University of Waterloo, Canada.

Krzysztof A. Kowal

K. Kowal is a fifth-year graduate student in the Department of Materials Science and Engineering of University of Pennsylvania. He is pursuing his Ph.D. degree working on atomic force microscopy investigations of surface structure changes during mechanical deformation and corrosion of aluminum-copper alloys.

K. Kowal received his master degree in physics from Jagiellonian University, Krakow, Poland, in July 1990. He specialized in solid state and computer physics. His master thesis was on the resisto-metric properties of a shape memory alloy - NiTi. After receiving a master degree, he worked until July 1991 in the Phase Transformation Kinetics Laboratory at Jagiellonian University. His research interests included computer modeling of SRO, LRO and decomposition kinetics. In May 1991 he was accepted as a candidate for Ph.D. at Department of Material Science and Engineering of University of Pennsylvania.

His current research interests include: electrochemistry, *in situ* electrochemical investigations by atomic force microscopy, and corrosion fatigue behavior of aluminum alloys. In May 1993, he participated in the 183rd Meeting of the Electrochemical Society at which he presented a paper on "*In Situ* Atomic Force Microscopy Study of the Plating and Stripping of Silver". In November 1993, he gave a presentation during the local meeting of the Philadelphia Section of the Electrochemical Society on "Studies of Electrochemical Processes by *In Situ* Atomic Force Microscopy". In May 1995, he participated in the 187th Meeting of the Electrochemical Society at which he presented a paper on "*In Situ* Atomic Microscopy Studies of Corrosion and Fatigue Behavior of Aluminum Copper Alloys".

RELEVANT PUBLICATIONS FROM THIS WORK

Journal of the Electrochemical Society, Vol. 143, No. 8, August 1996, p. 2471.

Materials Research Society Symposium Proceedings, Vol. 409, 1996, p. 201.